TECHNICAL PAPER

Micro liquid rotor operated by surface-acoustic-wave

**Tsunemasa Saiki · Katsuhide Okada ·
Yuichi Utsumi**

Abstract A micro liquid rotor operated by surface acoustic waves (SAWs) was proposed and fabricated. The liquid rotor has two interdigital transducers (IDTs) that generate SAWs, in order to increase efficiency of rotating the liquid. The IDTs were fabricated by patterning Al/Cr on a LiNbO$_3$ substrate. Moreover, the liquid rotor has a cylindrical liquid pool of 4 mm diameter and 200 μm depth. A sidewall of the liquid pool was made of epoxy-based negative photoresist on the substrate. As characteristics of the liquid rotor, we investigated relationships between electric power applied to the IDTs and angular velocity of the liquid or its temperature. Through experimentation, it was shown that the angular velocity and the temperature increase with increasing the electric power. When the fabricated liquid rotor was applied electric power of 2 W, the liquid of 5 μL rotated at 330 rad/s (3,100 rpm) and its temperature reached 65°C.

1 Introduction

Recently, micro total analysis systems (μTASs) have received a lot of attention in areas such as environment measurement and medical treatment. Reasons for this include these systems' efficiency in producing reactions, in thermal control, and in reducing the used amount of reagents as a result of miniaturization of the system. Furthermore, especially in μTAS called lab-on-a-chip, the manufacturing process of each device must be simplified in order to integrate many small devices such as pumps, valves, reactors, sensors, etc. on one chip.

Actuators and sensors that are used with surface acoustic waves (SAWs) that propagate along the surface of an elastic body have been reported (Andle et al. 1994; Chono et al. 2004; Galopin et al. 2006; Ito et al. 2007; Kondoh et al. 2003; Kurosawa et al. 1996; Renaudin et al. 2005; Shiokawa et al. 2004; Sritharan et al. 2006; Sroyanov et al. 2005; Utsumi et al. 2008; Wixforth 2003; Yamamoto et al. 2005). When an object is put on a propagating surface, the object moves and the SAWs attenuate. SAW actuators and SAW sensors are affected by this tendency. The SAWs are generated by applying a high-frequency voltage to an interdigital transducer (IDT). The IDT is fabricated simply by the patterning of an electrode on a piezoelectric substrate, making its structure very simple. Therefore, SAW actuators and SAW sensors are suitable for applications used in micro systems such as μTAS.

In liquid flow actuators operated by SAWs, water droplet moving had been mainly reported (Galopin et al. 2006; Renaudin et al. 2005; Wixforth 2003; Yamamoto et al. 2005), and there had been no reports of continuous liquid flow actuators. However, we fabricated a SAW drive pump and succeeded in creating a continuous flow of liquid (Utsumi et al. 2008). On the other hand, when the mixer operated by SAWs is focused on, there is a report that a water droplet put in the open space is rotated and mixed (Galopin et al. 2006). In not the open space but the enclosed space such as a flow channel, a liquid pool and so on, it seem to achieve the high mixing efficiency of liquid, because we can easily fix the liquid of the given quantity at the confined space.

T. Saiki (✉)
Department of Ecological and Biological Technologies,
Hyogo Prefectural Institute of Technology (HIT),
3-1-12 Yukihira, Suma, Kobe, Hyogo 645-0037, Japan
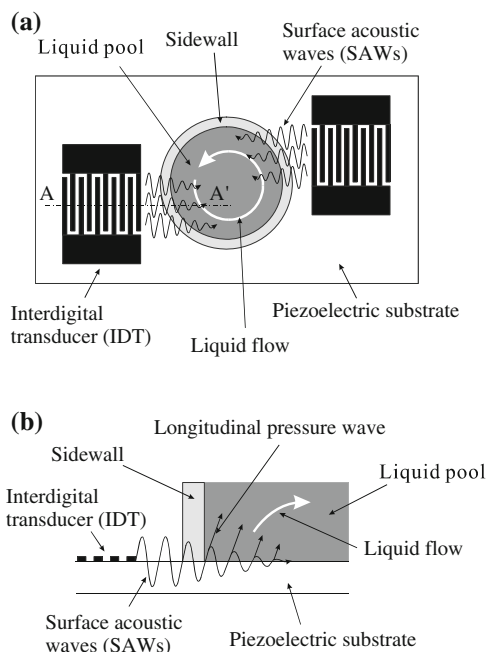e-mail: saiki@hyogo-kg.go.jp

T. Saiki · K. Okada · Y. Utsumi
Laboratory of Advanced Science and Technology for Industry
(LASTI), University of Hyogo, 3-1-2, Koto, Kamigori, Ako,
Hyogo 678-1205, Japan

Now, we take the enclosed-type rotating mixer in consideration, and propose a novel micro liquid rotor operated by SAWs. In this paper, we describe an overview of the liquid rotor, its fabrication method, and its physical property. Concretely, as the physical property, the relationship between the electric power applied to the IDTs of the liquid rotor and the rotation of the liquid in the pool is described. Furthermore, the relationship between the electric power and liquid temperature is also described, because there is a report that the temperature of the water droplet rises by SAWs (Ito et al. 2007).

2 Micro liquid rotor using SAWs

2.1 Design of micro liquid rotor

The top view and magnified sectional view of our micro liquid rotor are shown in Fig. 1a, b, respectively. When high frequency voltage is applied to a IDT, SAWs are generated from the IDT. The SAWs propagate in the surface layer of the substrate and pass through a sidewall to the plane of the liquid pool bottom. The liquid in the pool then becomes energized by longitudinal pressure wave radiation from the SAWs and flows in the propagated direction of the SAWs. Because the SAWs are incident in the direction that shifts parallel against the central axis of the pool, the liquid in the pool is rotated. Here, it was made to improve the rotation efficiency of the liquid by using two
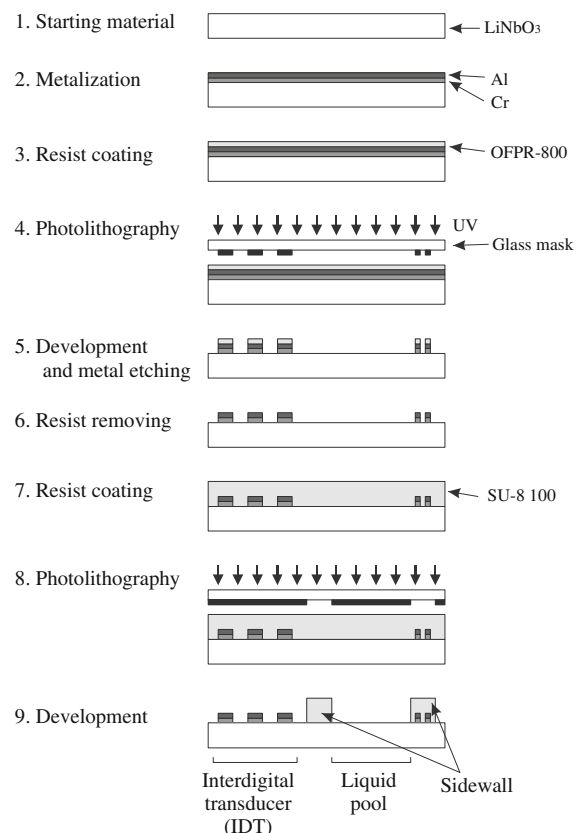
IDTs. On the other hand, the temperature of the liquid rises by the longitudinal pressure wave radiation simultaneously.
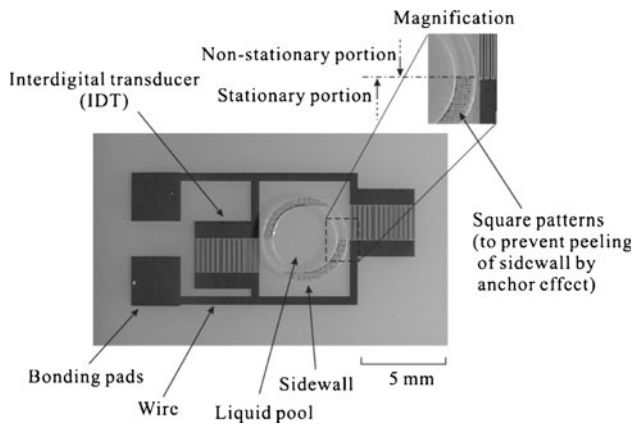
In our liquid rotor, to diversify the use of liquids, we developed an actuator structure in which the IDT and liquid do not directly come in contact with one another at the sidewall. In this structure, the upper parts of the IDT and the liquid pool are opened in order to attenuate the SAWs and to disturb the liquid flow.

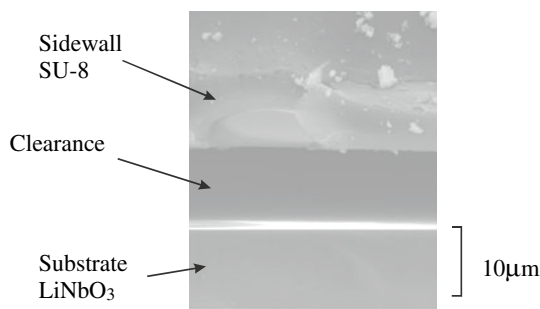### 2.2 Fabrication of micro liquid rotor

The fabrication procedure of the micro liquid rotor is shown in Fig. 2. First, a 50 nm Cr layer and a 1,000 nm Al layer were deposited on a piezoelectric substrate (127.8° y rotated x propagating LiNbO$_3$) by using RF sputter deposition. Next, positive photo resists (OFPR-800, Tokyo Ohka CO., LTD.) were spin-coated on the substrate with two metal layers, and the IDT electrode pattern of the glass mask was transferred to the resists by using UV lithography. By using this transcriptional pattern, the electrode of the IDT was produced by etching Al and Cl. Finally, the sidewall of the liquid pool was fabricated by UV lithography. The sidewall is made of epoxy-based negative photoresist (SU-8 100, MicroChem CO.). The height of the sidewall, i.e. the depth of the liquid pool, is approximately 200 μm.

Fig. 1 Overview of micro liquid rotor operated by SAWs. **a** Top view, **b** magnified sectional view (A–A')

Fig. 2 Fabrication procedure of micro liquid rotor

**Fig. 3** Photograph of fabricated micro liquid rotor

Fig. 4 SEM image of clearance at SAW entrance

A photograph of the fabricated micro liquid rotor is shown in Fig. 3. The liquid rotor consists of two parts of electric circuit such as IDT, bonding pads and so on, and liquid pool formed by the sidewall. At sidewall bottom in which the SAWs aren't incident, the 50 μm square patterns of Cr/Al are placed in order to prevent the peeling of the sidewall by anchor effect. Incidentally, when the first time the SAWs are generated on the chip, the sidewall part of SAW entrance is peeled off the substrate and tiny clearance of approximately 10 μm is formed between the sidewall and the substrate as shown in Fig. 4. Thereafter, the SAW whose amplitude is several hundred nm can pass through the clearance, but the liquid cannot passes through the clearance by the surface tension.

3 Rotational characteristic of micro liquid rotor operated by SAW

3.1 Experimental setup

As a rotational characteristic of the micro liquid rotor, we investigated angular velocity of the liquid. Our experimental setup for measuring angular velocity of liquid is shown in Fig. 5. Before starting the experiment, a liquid pool of a round shape of 4 mm diameter was filled with 5 μL. In the experiment, a function generator (AFG3252,
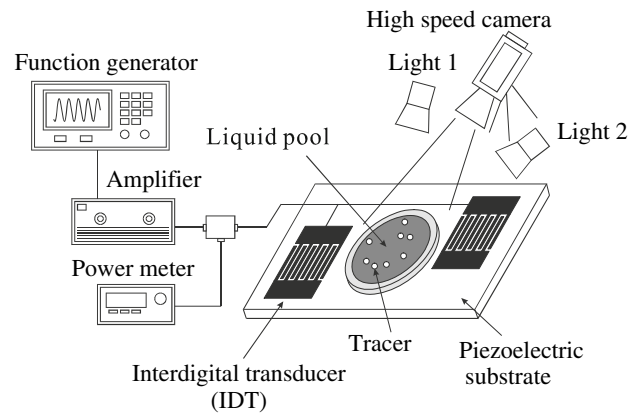

Fig. 5 Experimental setup for measuring angular velocity of liquid

Tektronix Co.) generated high frequency voltage, and the voltage was amplified with an amplifier (ARF15237-25, ASTEC Co.). Here, as the high frequency voltage, we used 1 kHz burst waveform consisted of 1,000 cycles of sine wave of 19.2 MHz, in order to prevent damage to the piezoelectric substrate by the generation of heat. The SAWs were generated by applying this amplified voltage to the two IDTs. For IDT parameters, we used a stripline pitch of 200 μm, 20 stripline pairs and an aperture size of 2 mm, which was the same as the liquid pool radius r, by reference to our previous reports (Utsumi et al. 2008). Here, we measured not the applied voltage to IDTs, but the electric power P by the RF power meter (NRP-Z91, Rohde & Schwarz K.K. and DC3001M1, AR Co.). The SAWs propagate in the surface layer of the substrate and pass through a sidewall to the plane of the liquid pool bottom. Finally, the liquid in the pool is rotated. The rotational characteristics were recorded using a high-speed camera (MEMRECAM fx-K3, nac Image Technology, Inc.). In order to obtain necessary light intensity for photographing by the high speed camera, two tungsten halogen lighting (ARRILIRE600, ARRI Inc.) were used. For the flow visualization of the liquid, organic dye (Orange II: $C_{16}H_{11}N_2NaO_4S$) was dissolved by deionized water as liquid. The liquid has a volume ratio of 200 deionized water to one organic dye. Additionally, Al particles were added to the liquid. From sequential photographs taken by the high speed camera, the angular velocity ω of liquid rotation was measured using positions of tracers of Al particles.

3.2 Results

The sequential photographs at the liquid pool in time of applying the electric power to the IDTs are shown in Fig. 6. Here, Fig. 6a–f are six photographs taken in 10 ms interval at 3.00–3.05 s after the electric power of 350 mW was applied to the IDTs. White circles in these figures show the positions of the same tracer, and the circles are drawn in order to recognize movement of one tracer. Thus, it is possible to
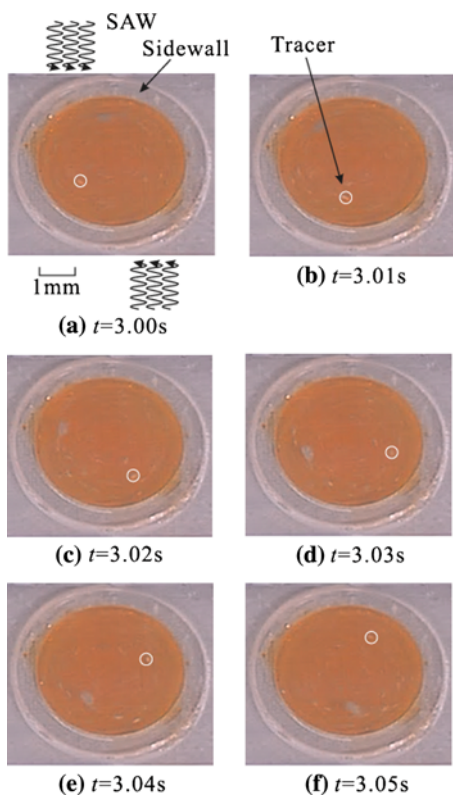
Fig. 6 Sequential photographs taken by high speed camera at liquid pool. (electric power: 350 mW)

observe that the tracer circulate in a counterclockwise direction with elapsed time t. When all tracer is observed, it is found that the liquid of the pool rotates. Incidentally, SAWs propagate down form top left position and propagate up from bottom right position in each Figure (See Fig. 6a).

Then, the angular velocity of the liquid rotation is measured from the high speed sequential photographs. Firstly we obtain a time interval $\Delta t = t_b - t_a$ in which a tracer located about $3r/4$ from the liquid pool center moves $\pi/4$ rad, i.e. from point A to point B (See Fig. 7), where r is the diameter of the liquid pool circle. Secondly, an angular velocity ω is calculated from the time interval Δt and the moving angle ($\pi/4$) of the tracer.
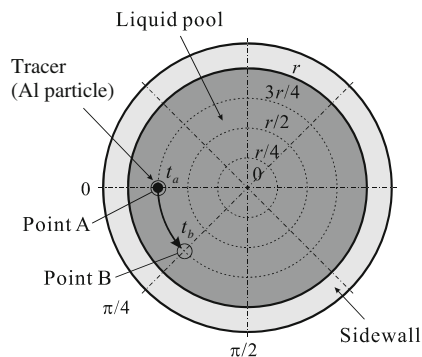

Fig. 7 Calculation method of angular velocity of liquid rotation
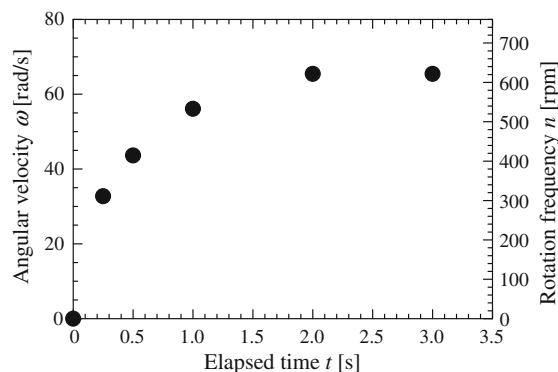
Fig. 8 Temporal change of angular velocity of liquid rotation

The temporal change of the angular velocity of the liquid rotation is shown in Fig. 8. The horizontal axis and vertical axis represent the elapsed time t since the start of applying electric power to the IDTs and the angular velocity ω (or rotation frequency n) of the liquid in the pool, respectively. Here, the electric power P was 347 mW. As seen in Fig. 8, the angular velocity of liquid rotation rapidly increased with an increase of elapsed time. Then, the angular velocity reached maximum value after about 2 s. Here, if a final angular velocity of pulse response is 65 rad/s at elapsed time 2 s, the time constant is 0.47 s. From these results, we guess that the response time of the angular velocity in the fabricated micro liquid rotor is a few seconds.

Next, relationship between the electric power applied to the IDT and the angular velocity of liquid rotation is shown in Fig. 9. Here, the elapsed time t is 3 s after the electric power was applied to the IDT. The horizontal axis and the vertical axis represent the electric power P and the angular velocity ω, respectively. The dotted line is drawn by calculation of the least squares method. As seen in Fig. 9, the liquid began to rotate at about 100 mW. The angular velocity increased with an increase of the electric power, and the maximum angular velocity of our fabricated liquid rotor was about 330 rad/s (3,100 rpm) at 2,030 mW. Incidentally, when applied electric power to the rotor was 3 W, we
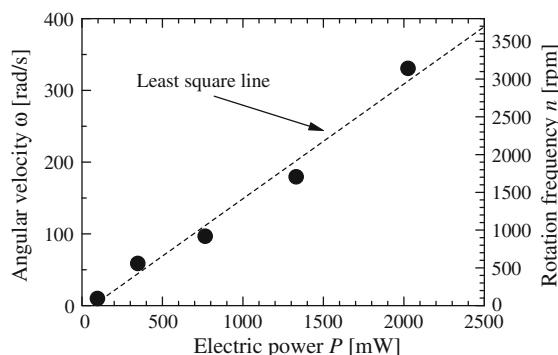
Fig. 9 Relationship between electric power applied to IDT and angular velocity of liquid rotation

observed that the liquid in the pool was not only rotated but also splattered outside by atomization. Thus, the micro liquid rotor operated by SAWs has an applied electric power range that is suitable for producing a rotation of liquid.

4 Temperature rise characteristic of micro liquid rotor operated by SAW

4.1 Experimental setup

Our experimental setup for measuring temperature rise of liquid in the micro liquid rotor is shown in Fig. 10. These experimental equipments are about the same as those explained in previous section. However, in order to measure temperature T of the liquid, an infrared thermography camera (Neo Thermo TVS-700, Avionics Co.) instead of a high speed camera was used. In the experiment, the liquid pool was filled with 5 μL of deionized water.

4.2 Results

Thermal images of the micro liquid rotor in applying electric power to the IDTs are shown in Fig. 11a–g. These thermal images are taken at $t = 0, 1, 2, 5, 10, 20$, and 30 s after electric power P of 1,330 mW was applied to the IDTs. The temperature scale of these images is shown only in right side of Fig. 11g. As seen in Fig. 11a, temperatures both water in liquid pool and sidewall are about 23°C at $t = 0$ s, and those are almost equal to the room temperature. The temperature around the sidewall was raised at 1 s after the starting point of operation of the SAW as seen in b, and the temperature of the water in the liquid pool was raised at 2 s after as seen in c. Moreover, the temperature of the water became about 55°C at 30 s after the electric power was applied to IDTs as seen in g. From these results, it is proven that the temperature of the liquid increases with an increase of the elapsed time. On the other hand, when these figures are individually observed, it is shown that the
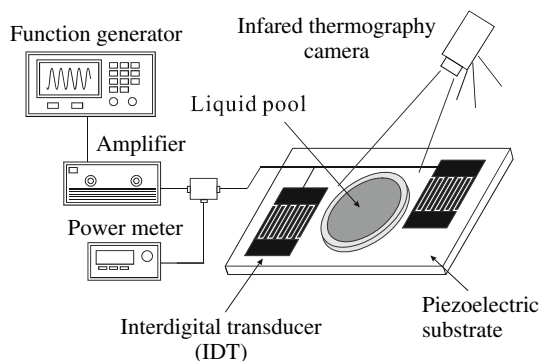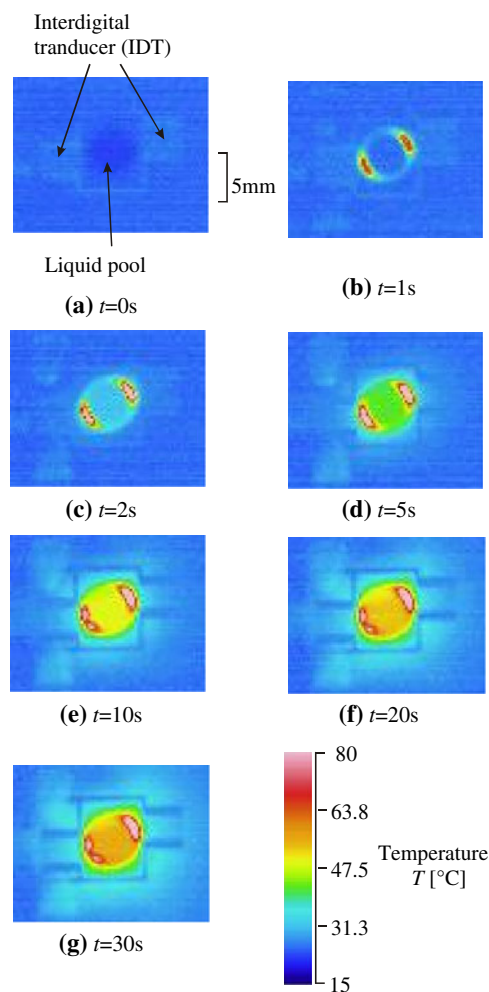

Fig. 11 Thermal images of micro liquid rotor. (Electric power: 1,330 mW)

temperatures of the liquid are spatially uniform distributions of the liquid in each elapsed time. We gasses that the spatially uniform distribution is occurred by rapid mixing with high-speed rotation of the liquid.

Next, temporal changes of the liquid temperature are shown in Fig. 12. The horizontal axis and vertical axis represent the elapsed time t and the temperature T, respectively. The open triangles, filled circles, open circles, filled quadrangles and open quadrangles represent applied electric power P of 100, 350, 770, 1,330 and 2,030 mW, respectively. As seen in Fig. 12, the temperature of the liquid rapidly increased with an increase of elapsed time after the electric power was applied to the IDT. Then, it begins to gradually saturate the temperature of the liquid at about 10 s after. From these results, we guess that the response time of the temperature of the liquid in the fabricated micro liquid rotor is a few dozen seconds. This temperature response time is slower than the angular velocity response time mentioned in section of 3.2. On the

Fig. 10 Experimental setup for measuring temperature rise of liquid
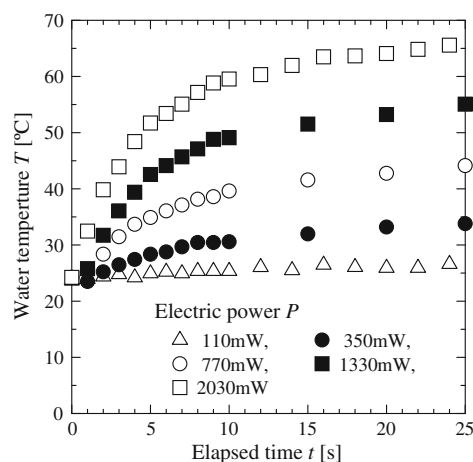
Fig. 12 Temporal changes of liquid temperature

other hands, the temperature of the liquid rises with that electric power is large at all elapsed time. Incidentally, when the fabricated liquid rotor was applied electric power of 2,030 mW, the temperature of the liquid in the pool reached 65°C at 25 s after. The achieved static temperature increase should be the result of the competition of input and output of the heat flux. Therefore, the real temperature increase was supposed to be higher than the measured temperature. Precise investigation of thermohydrodynamic performance of the liquid rotor should be remain necessary in the work.

5 Conclusions

We take the enclosed-type rotating mixer in consideration, and propose the novel micro liquid rotor operated by SAWs. The fabricated micro liquid rotor has a cylindrical liquid pool (a diameter of 4 mm and a depth of 200 μm) and two IDTs (a stripline pitch of 200 μm, 20 stripline pairs and an aperture size of 2 mm) in order to increase efficiency of rotating the liquid. Because the SAWs generated by applying high frequency voltage to the IDTs are incident in the direction that shifts parallel against the central axis of the pool, the liquid in the pool is rotated. The IDTs were fabricated by patterning Al/Cr on a LiNbO$_3$ substrate and a sidewall of the liquid pool was made of epoxy-based negative photoresist SU-8 on the substrate.

As characteristic of the fabricated micro liquid rotor, we investigated relationships between electric power applied to the IDTs and angular velocity of the liquid or its temperature. As a result, we found that the angular velocity and the temperature increase with increasing the electric power.

In addition, we found that a response time of the angular velocity is faster than that of temperature of the liquid too. When the fabricated liquid rotor was applied electric power of 2 W, the liquid of 5 μL rotated at 330 rad/s (3,100 rpm) and its temperature reached 65°C. Thus, we expect that the liquid rotor may be able to use such as not only mixer but alos thermal reactor and cyclone separator in μTAS.

References

Andle JC, Vetelino JF (1994) Acoustic wave biosensors. Sens Actuators A 44:167–176

Chono K, Shimizu N, Matsui Y, Kondoh J, Shiokawa S (2004) Development of novel atomization system based on SAW streaming. Jpn J Appl Phys 43:2987–2991. doi:10.1143/JJAP.43.2987

Galopin E, Renaudin A, Camart JC, Thomy V, Druon C, Tabourier P (2006) Enhanced protein capture by ultrafast SAW droplet μmixing. In: Proceedings of 10th international conference on miniaturized systems for chemistry and life Sciences (μTAS2006), pp 651–653

Ito S, Sugimoto M, Matsui Y, Kondoh J (2007) Study of surface acoustic wave streaming phenomenon based on temperature measurement and observation of streaming in liquids. Jpn J Appl Phys 46:4718–4722. doi:10.1143/JJAP.46.4718

Kondoh J, Muramatsu T, Nakanishi T, Matsui Y, Shiokawa S (2003) Development of practical surface acoustic wave liquid sensing system and its application for measurement of japanese tea. Sens Actuators B 92:191–198. doi:10.1016/S0925-4005(03)00263-6

Kurosawa M, Takahashi M, Higuchi T (1996) Ultrasonic linear motor using surface acoustic wave. IEEE Trans Ultrason Ferroelectr Freq Control 43:901–906

Renaudin A, Chuda K, Zhang V, Coqueret X, Camart JC, Tabourier P, Druon C (2005) SAW Lab-on-chip in view of protein affinity purification implemented from nanodroplet transport. In: Proceedings of 9th international conference on miniaturized systems for chemistry and life sciences (μTAS2005), pp 599–601

Shiokawa S, Kondoh J (2004) Surface acoustic wave sensors. Jpn J Appl Phys 43:2799–2802. doi:10.1143/JJAP.43.2799

Sritharan K, Strobl CJ, Schneider MF, Wixforth A (2006) Acoustic mixing at low Reynold's numbers. Appl Phys Lett 88: 054102. doi: 10.1063/1.2171482

Sroyanov I, Tewes M, Glass S, Gronewold T, Koch M, Lohndorf M (2005) Development of microfluidic interfaces for a surface acoustic wave (SAW) biosensor system. In: Proceedings of 9th international conference on miniaturized systems for chemistry and life sciences (μTAS2005), pp 1152–1154

Utsumi Y, Saiki T, Okada K (2008) Proposal of a novel continuous flow pumping operated by surface acoustic wave. In: Proceedings of 12th international conference on miniaturized systems for chemistry and life sciences (μTAS2008), pp 715–717

Wixforth A (2003) Acoustically driven planar microfluidics. Superlattices Microstruct 33:389–396

Yamamoto A, Nishimura A, Tsukada N, Higuchi T (2005) An integrated droplet manipulation device using surface acoustic wave. In: Proceedings of 9th international conference on miniaturized systems for chemistry and life sciences (μTAS2005), pp 1072–1074